

## Graphical Abstract

### **Synaptic Pruning: A Biological Inspiration for Deep Learning Regularization**

Gideon Vos, Liza van Eijk, Zoltan Sarnyai, Mostafa Rahimi Azghadi

## Synaptic Pruning: A Biological Inspiration for Deep Learning Regularization



Dropout regularization improves generalization by randomly deactivating neurons during training.



We propose a method using activity-dependent node pruning as a direct substitute for standard dropout layers.



Results show a 20% reduction in Mean Absolute Error compared to alternative regularization techniques.



Our biologically-inspired approach particularly excels in financial time series forecasting applications.

## Highlights

### **Synaptic Pruning: A Biological Inspiration for Deep Learning Regularization**

Gideon Vos, Liza van Eijk, Zoltan Sarnyai, Mostafa Rahimi Azghadi

- We propose a magnitude-based synaptic pruning method as a regularization approach
- The method emulates biological synaptic pruning by dynamically and progressively eliminating low-importance neural connections
- Experiments across RNN, LSTM, and PatchTST models show statistically significant error reductions
- Our approach reduces predictive error rates by up to 52% in times series forecasting tasks

# Synaptic Pruning: A Biological Inspiration for Deep Learning Regularization

Gideon Vos<sup>a</sup>, Liza van Eijk<sup>b</sup>, Zoltan Sarnyai<sup>c</sup>, Mostafa Rahimi Azghadi<sup>a</sup>

<sup>a</sup>*College of Science and Engineering, James Cook University, James Cook Dr, Townsville, 4811, QLD, Australia*

<sup>b</sup>*College of Health Care Sciences, James Cook University, James Cook Dr, Townsville, 4811, QLD, Australia*

<sup>c</sup>*College of Public Health, Medical, and Vet Sciences, James Cook University, James Cook Dr, Townsville, 4811, QLD, Australia*

---

## Abstract

*Introduction.* Synaptic pruning is a key neuro-developmental process in biological brains that removes weak connections to improve neural efficiency. In artificial neural networks, standard dropout regularization randomly deactivates neurons during training but overlooks the activity-dependent nature of biological pruning. This study proposes a novel regularization method that better reflects biological pruning by gradually eliminating connections based on their contribution to model performance.

*Methods.* We propose a magnitude-based synaptic pruning approach that integrates directly into the training loop of deep learning models as a replacement for dropout layers. The method computes weight importance from absolute magnitudes across all layers, applying a cubic schedule to gradually increase global sparsity during training. At set intervals, pruning masks are updated by thresholding weights, permanently removing low-importance connections while retaining gradient flow for active weights. This continuous, data-driven pruning eliminates the need for separate pruning and fine-tuning phases.

*Results.* Experimental results across multiple time series forecasting deep neural network architectures, including Recurrent Neural Networks, Long Short Term Memory, and Patch Time Series Transformer on four different forecasting datasets demonstrate the efficacy of our synaptic pruning method.

The method achieved the best overall performance ranking across all architectures, with statistically significant improvements confirmed by Friedman tests ( $p < 0.01$ ) on all datasets. Notably, our proposed method achieves substantial improvements in financial forecasting tasks, reducing Mean Absolute Error by up to 20% compared to models using no dropout or standard dropout for regularization, with reductions reaching up to 52% in select transformer models.

*Conclusion.* The proposed synaptic pruning mechanism advances regularization by coupling dynamic weight elimination with progressive sparsification during training. Its ease of integration with diverse architectures, coupled with superior forecasting accuracy, underscores its potential as a practical alternative to other dropout techniques, especially in domains like financial time series forecasting, where precision and efficiency are critical.

*Keywords:* Machine Learning, Neuroscience, Regularization

*PACS:* 07.05.Mh, 87.19.La

*2000 MSC:* 68T01, 92-08

---

## 1. Introduction

Synaptic pruning is a fundamental neuro-developmental process whereby weak or redundant synaptic connections are selectively eliminated to enhance the efficiency of neuronal networks [1]. This process is highly activity-dependent, meaning that synapses with lower activity or utility are more likely to be pruned, resulting in improved energy efficiency and functional specialization [2]. During critical periods of development, the human brain initially overproduces synapses, creating a dense network of connections that undergoes substantial refinement through adolescence and early adulthood [3, 4]. This refinement is essential for optimal cognitive function and normal brain development, with disruptions in pruning mechanisms associated with various neuro-developmental disorders [5, 6].

In the field of artificial neural networks, researchers have drawn inspiration from biological synaptic pruning to develop methods for improving network efficiency and generalization capacity [7–9]. Dropout regularization [10] functions by randomly deactivating, or "dropping out," a subset of neurons during each training iteration. This process forces the network to avoid over-reliance on any particular neuron, promoting redundancy and robustness in

the learned representations. By preventing neurons from co-adapting too strongly to specific patterns in the training data, dropout reduces the risk of overfitting. As a result, the model is encouraged to generalize better to unseen data, leading to improved performance during inference. More recent approaches have extended beyond dropout to implement more biologically-inspired pruning methods that permanently remove weights or connections based on importance criteria [9, 11], potentially offering advantages in both computational efficiency and performance.

In this work, we introduce a novel regularization method that more closely emulates biological synaptic pruning within deep neural networks, with a particular focus on enhancing time series forecasting performance. Unlike standard dropout, which randomly and temporarily deactivates neurons during training, or pruning techniques aimed solely at post-training model compression, our method applies an activity-dependent, gradual elimination of connections based on their contribution to model performance [12]. By combining temporal scheduling with context-sensitive pruning, our approach progressively weakens and permanently removes low-importance connections during training, enabling the network to adapt dynamically. By integrating directly into the training process, our method requires no additional pruning or fine-tuning stages and is especially effective in recurrent and temporal models commonly used for time series forecasting.

## 2. Related Works

In computational neuroscience and deep learning, several methods have been proposed to emulate biological synaptic pruning. LeCun *et al.* proposed Optimal Brain Damage [7], one of the earliest approaches to biologically inspired pruning in artificial neural networks. This method uses second-order derivatives of the loss function to estimate the saliency of each weight, pruning those with minimal impact on performance. However, this approach requires complete model training before pruning begins, making it a post-training optimization rather than an integrated learning process that could adapt to evolving temporal patterns in time series data.

Han et al. [9] introduced magnitude-based pruning, where neural network weights with magnitudes below a certain threshold are eliminated, under the assumption that they contribute less to the final output. While effective in

reducing network complexity, this approach primarily focuses on static weight values and does not consider the dynamic importance of individual nodes or features over time, which is particularly limiting for time series forecasting where temporal dependencies change throughout the learning process. This approach further requires three independent steps consisting of initial model training, pruning, and finally model fine-tuning, making it less practical for applications where continuous adaptation during training is valuable.

Li et al. [13] proposed sensitivity-based pruning for Convolutional Networks, also known as contribution-aware pruning, which evaluates the increase in loss when individual neurons are ablated, thereby preserving units that significantly impact performance. This method aligns with the biological concept of activity-dependent synaptic retention, where synapses that contribute more to network function are retained, while those with minimal impact are pruned. However, this approach still operates through discrete evaluation phases rather than continuous monitoring, which may miss the evolving importance of features during model training and inference.

Gradient-based pruning was proposed by Molchanov et al. [11], which analyzes the gradient flow through each neuron or connection and prunes those with consistently low gradient magnitudes, indicating minimal contribution to loss reduction. While this approach captures some dynamic behavior of the network, it often incurs high computational overhead due to the need to calculate gradients for every neuron or connection during training, and typically requires separate pruning phases distinct from regular training.

Hassabis et al. [8] presented a broader framework linking neuroscience and artificial intelligence, emphasizing how mechanisms such as synaptic pruning and activity-dependent plasticity inform efficient computation in the brain. They argued that integrating biological principles into artificial systems, such as pruning underused or redundant connections, can lead to more robust, adaptable, and generalizable models. This perspective supports pruning not merely as a compression technique, but as a fundamental principle for learning and generalization, grounded in neuro-biological theory, which is particularly relevant for time series forecasting where adaptability to changing patterns is crucial.

Frankle et al. [12] introduced the Lottery Ticket Hypothesis (LTH), which

suggests that within large networks exist sparse sub-networks, referred to as “winning tickets,” that can achieve comparable performance if identified early and pruned effectively. LTH finds inherently trainable sparse architectures that require retraining from specific initial conditions. This approach mimics developmental pruning by identifying and retaining strong sub-networks early in training, much like how the brain strengthens key neural connections during development while pruning others. However, the iterative process of training, pruning, and retraining may be less practical for applications where continuous adaptation during a single training cycle is preferred.

Gradient-based Single-shot Pruning (SNIP) was introduced by Lee *et al.* [14], which estimates the importance of each connection at initialization by measuring the sensitivity of the loss to small perturbations in the weights. Connections with low gradient-based saliency scores are pruned before training begins, under the assumption that their contribution to learning will remain negligible. While computationally efficient, this approach makes one-time pruning decisions based on the network’s initial state, assuming that early indicators reliably predict long-term relevance, which may not hold for cases where feature importance can evolve as the model learns different temporal patterns.

Wang *et al.* [15] proposed Gradient Signal Preservation (GraSP), aiming to maintain trainability in pruned networks by preserving the gradient flow at initialization. GraSP evaluates the influence of each weight on the network’s Hessian-gradient product and prunes connections that minimally affect gradient propagation. This method improves over naive pruning by considering second-order interactions. However, like SNIP, it makes static pruning decisions at initialization rather than adapting to changing feature importance throughout training, which limits its effectiveness when temporal relationships may shift during the learning process.

In contrast to these existing approaches, our proposed method operates as a potential replacement or augmentation for standard dropout during training, continuously monitoring and updating connection importance based on their contribution to reducing prediction error. While preliminary experiments with computer vision architectures, including EfficientNet, DenseNet, and VGG, showed minimal efficacy, this dynamic, activity-dependent approach proved particularly well-suited for time series forecasting applications where

temporal patterns and feature relevance can evolve as the model learns, and where the ability to identify and preserve the most predictive temporal relationships throughout training is crucial for achieving optimal performance.

### 3. Methods

#### 3.1. Proposed Pruning Method

The method proposed in this study implements a global magnitude-based weight pruning strategy that progressively removes connections based on their importance to the network’s predictive performance. Our synaptic pruning approach differs fundamentally from standard dropout [10] and other regularization techniques in several key aspects. Specifically, our method:

- Employs global magnitude-based pruning across all network layers simultaneously
- Implements a cubic scheduling function for gradual sparsity increase over training epochs
- Maintains binary masks that permanently remove connections rather than stochastic deactivation
- Uses a warmup period to allow initial weight development before pruning begins
- Results in a structurally sparse network with reduced computational requirements

Our proposed method operates at the individual weight level using global magnitude comparison, ensuring that only the least important connections across the entire network are removed. This approach aligns well with biological synaptic pruning principles where weaker synaptic connections are eliminated to optimize neural efficiency [16–18].

#### 3.2. Pruning Components

The synaptic pruning algorithm consists of three main components: i) mask initialization, ii) cubic sparsity scheduling, and iii) global magnitude-based selection.

### 3.2.1. Mask Initialization

Upon initialization, binary masks are created for all weight parameters in the fully connected layers. These masks are initialized as binary tensors.

### 3.2.2. Cubic Sparsity Scheduling

The target sparsity follows a cubic scheduling function that enables gradual pruning progression. After a warmup period of 2 epochs (adjustable as a parameter), the sparsity increases from a minimum rate of 30% to a maximum of 70% according to:

$$s(t) = s_{\min} + (s_{\max} - s_{\min}) \cdot \left( \frac{t_{\text{total}} - t_{\text{warmup}}}{t - t_{\text{warmup}}} \right)^3$$

where  $s(t)$  is the target sparsity at epoch  $t$ ,  $s_{\min} = 0.3$ ,  $s_{\max} = 0.7$ ,  $t_{\text{warmup}} = 2$ , and  $t_{\text{total}} = 20$ .

### 3.2.3. Global Magnitude-based Selection

The core pruning mechanism evaluates all active (non-pruned) weights across the network simultaneously. At each pruning step, our method:

- Collects all currently active weights from all modules
- Calculates the absolute magnitude of each weight
- Determines a global threshold based on the target number of weights to prune
- Updates masks to zero out weights below the threshold
- Applies the updated masks to preserve the pruned structure

This global selection ensures that pruning decisions consider the relative importance of weights across different layers, preventing any single layer from being over-pruned while others remain dense.

## 3.3. Training Integration

The proposed pruning method is integrated into the usual training loop of deep neural networks, with pruning applied every 5 batches (after the initial warmup period), allowing for frequent adaptation to changing weight

importance. The pruning masks are applied both immediately after pruning updates and after each optimizer step to ensure pruned weights remain at zero. The six key algorithms utilized for synaptic pruning are shown as pseudo-code below, with the full implementation provided as Python source code available at <https://github.com/xalentis/SynapticPruning>.

---

**Algorithm 1** Synaptic Pruning Initialization

---

**Require:** Neural network modules  $\mathcal{M} = \{M_1, M_2, \dots, M_k\}$   
**Require:** Minimum sparsity rate  $s_{min} = 0.3$   
**Require:** Maximum sparsity rate  $s_{max} = 0.7$   
**Require:** Warmup epochs  $t_{warmup} = 2$   
**Require:** Total training epochs  $t_{total} = 20$   
**Ensure:** Initialized binary masks  $\mathcal{B}$

- 1: Initialize empty mask dictionary  $\mathcal{B} \leftarrow \{\}$
- 2: **for** each module  $M_i \in \mathcal{M}$  **do**
- 3:   **for** each parameter  $\theta \in M_i$  where  $\theta$  is a weight tensor **do**
- 4:     Create binary mask  $B_\theta \leftarrow \mathbf{1}_{|\theta|}$  {Initialize all weights as active}
- 5:      $\mathcal{B}[\theta] \leftarrow B_\theta$
- 6:   **end for**
- 7: **end for**
- 8: **return**  $\mathcal{B}$

---



---

**Algorithm 2** Cubic Sparsity Scheduling

---

**Require:** Current epoch  $t$   
**Require:** Warmup epochs  $t_{warmup} = 2$   
**Require:** Total epochs  $t_{total} = 20$   
**Require:** Minimum sparsity  $s_{min} = 0.3$   
**Require:** Maximum sparsity  $s_{max} = 0.7$   
**Ensure:** Target sparsity  $s(t)$

- 1: **if**  $t < t_{warmup}$  **then**
- 2:   **return**  $s(t) = 0.0$
- 3: **end if**
- 4:  $progress \leftarrow \frac{t - t_{warmup}}{t_{total} - t_{warmup}}$
- 5:  $progress \leftarrow \min(1.0, \max(0.0, progress))$
- 6:  $s(t) \leftarrow s_{min} + (s_{max} - s_{min}) \cdot progress^3$
- 7: **return**  $s(t)$

---

---

**Algorithm 3** Global Magnitude-Based Weight Selection

---

**Require:** Binary masks  $\mathcal{B}$

**Require:** Neural network modules  $\mathcal{M}$

**Require:** Target sparsity  $s_{target}$

**Ensure:** Updated masks  $\mathcal{B}'$

```
1: Initialize empty lists:  $W_{active} \leftarrow []$ ,  $P_{info} \leftarrow []$ 
2: for each module  $M_i \in \mathcal{M}$  do
3:   for each weight parameter  $\theta \in M_i$  do
4:      $B_\theta \leftarrow \mathcal{B}[\theta]$  {Get current mask}
5:      $I_{active} \leftarrow$  indices where  $B_\theta = 1$ 
6:      $W_{active\_weights} \leftarrow |\theta[I_{active}]|$  {Absolute magnitudes of active weights}
7:     if  $|W_{active\_weights}| > 0$  then
8:        $W_{active}.\text{append}(W_{active\_weights})$ 
9:        $P_{info}.\text{append}((\theta, I_{active}))$ 
10:      end if
11:    end for
12:  end for
13: if  $W_{active}$  is empty then
14:   return  $\mathcal{B}$ 
15: end if
16:  $W_{all} \leftarrow \text{concatenate}(W_{active})$ 
17:  $n_{total} \leftarrow \sum_{\theta, I} |\theta|$  for all  $(\theta, I) \in P_{info}$ 
18:  $n_{active} \leftarrow |W_{all}|$ 
19:  $n_{target\_pruned} \leftarrow \lfloor s_{target} \cdot n_{total} \rfloor$ 
20:  $n_{currently\_pruned} \leftarrow n_{total} - n_{active}$ 
21:  $n_{additional\_prune} \leftarrow \max(0, n_{target\_pruned} - n_{currently\_pruned})$ 
22: if  $n_{additional\_prune} = 0$  OR  $n_{additional\_prune} \geq n_{active}$  then
23:   return  $\mathcal{B}$ 
24: end if
25:  $\tau \leftarrow \text{kthvalue}(W_{all}, n_{additional\_prune})$  {Find pruning threshold}
26: for each  $(\theta, I_{active}) \in P_{info}$  do
27:    $B'_\theta \leftarrow \mathcal{B}[\theta].\text{clone}()$ 
28:    $W_{prune\_mask} \leftarrow |\theta[I_{active}]| < \tau$ 
29:   for each position  $pos$  in  $I_{active}$  where  $W_{prune\_mask}[pos] = \text{True}$  do
30:      $B'_\theta[pos] \leftarrow 0$  {Prune weight}
31:   end for
32:    $\mathcal{B}[\theta] \leftarrow B'_\theta$ 
33: end for
34: return  $\mathcal{B}$ 
```

---

---

**Algorithm 4** Synaptic Pruning Training Integration

---

**Require:** Training dataset  $\mathcal{D}$   
**Require:** Neural network model  $f_\theta$   
**Require:** Optimizer  $\mathcal{O}$   
**Require:** Loss function  $\mathcal{L}$   
**Require:** Pruning frequency  $f_{prune} = 5$  batches  
**Require:** Total epochs  $E$   
**Ensure:** Trained model  $f_{\theta^*}$  with sparse structure

- 1: Initialize synaptic pruning masks  $\mathcal{B}$  {Algorithm 1}
- 2:  $batch\_count \leftarrow 0$
- 3: **for** epoch  $e = 1$  to  $E$  **do**
- 4:   **for** each batch  $(X, y) \in \mathcal{D}$  **do**
- 5:      $batch\_count \leftarrow batch\_count + 1$
- 6:     // Forward pass
- 7:      $\hat{y} \leftarrow f_\theta(X)$
- 8:      $loss \leftarrow \mathcal{L}(\hat{y}, y)$
- 9:     // Backward pass
- 10:     $\mathcal{O}.zero\_grad()$
- 11:     $loss.backward()$
- 12:    // Pruning update (every  $f_{prune}$  batches after warmup)
- 13:    **if**  $e \geq t_{warmup}$  AND  $batch\_count \bmod f_{prune} = 0$  **then**
- 14:       $s_{target} \leftarrow \text{CubicSchedule}(e)$  {Algorithm 2}
- 15:       $\mathcal{B} \leftarrow \text{GlobalMagnitudePruning}(\mathcal{B}, s_{target})$  {Algorithm 3}
- 16:    **end if**
- 17:    // Optimizer step
- 18:     $\mathcal{O}.step()$
- 19:    // Apply masks to ensure pruned weights remain zero
- 20:     $\text{ApplyMasks}(\theta, \mathcal{B})$
- 21:   **end for**
- 22: **end for**
- 23: **return**  $f_{\theta^*}$

---

---

**Algorithm 5** Apply Pruning Masks

---

**Require:** Model parameters  $\theta$

**Require:** Binary masks  $\mathcal{B}$

**Ensure:** Updated parameters with pruned connections set to zero

```
1: for each weight parameter  $w \in \theta$  do
2:   if  $w \in \mathcal{B}$  then
3:      $B_w \leftarrow \mathcal{B}[w]$ 
4:      $w \leftarrow w \odot B_w$  {Element-wise multiplication to zero out pruned
   weights}
5:   end if
6: end for
```

---

---

**Algorithm 6** Sparsity Statistics Computation

---

**Require:** Binary masks  $\mathcal{B}$

**Require:** Neural network modules  $\mathcal{M}$

**Ensure:** Sparsity statistics  $\mathcal{S}$

```
1: Initialize statistics dictionary  $\mathcal{S} \leftarrow \{\}$ 
2:  $layer\_idx \leftarrow 0$ 
3: for each module  $M_i \in \mathcal{M}$  do
4:   for each weight parameter  $\theta \in M_i$  do
5:      $B_\theta \leftarrow \mathcal{B}[\theta]$ 
6:      $n_{total} \leftarrow |B_\theta|$  {Total number of weights}
7:      $n_{pruned} \leftarrow \sum_j (B_\theta[j] = 0)$  {Number of pruned weights}
8:      $sparsity \leftarrow \frac{n_{pruned}}{n_{total}}$ 
9:      $key \leftarrow M_i.class\_name + " - " + \theta.name + " - " + layer\_idx$ 
10:     $\mathcal{S}[key] \leftarrow \{$ 
11:      'total_weights' :  $n_{total}$ ,
12:      'pruned_weights' :  $n_{pruned}$ ,
13:      'sparsity' :  $sparsity$ 
14:    }
15:  end for
16:   $layer\_idx \leftarrow layer\_idx + 1$ 
17: end for
18: return  $\mathcal{S}$ 
```

---

### 3.4. Biological Inspiration

This approach mirrors biological synaptic pruning processes observed in neural development, where initially overproduced synaptic connections are selectively eliminated based on their functional importance [16, 19, 20]. The gradual nature of our cubic scheduling function reflects the progressive refinement seen in biological neural networks, where pruning occurs over extended periods rather than through abrupt elimination. Additionally, the global magnitude-based selection mechanism ensures that only the most functionally relevant connections are preserved, similar to how biological systems maintain synapses that contribute most effectively to information processing and learning.

### 3.5. Comparison with Alternative Approaches

Unlike alternative dropout approaches [21, 22], which introduce learnable parameters and stochastic behavior, our method provides deterministic, magnitude-based pruning that results in genuinely sparse networks. This approach differs from methods like SNIP [14] by operating during training rather than at initialization, allowing for dynamic adaptation to learned representations. The global comparison strategy ensures more balanced pruning across layers compared to layer-wise approaches, leading to more efficient overall network architectures.

### 3.6. Implementation

When implemented on an LSTM architecture (Figure 1), standard dropout randomly deactivates neurons in the hidden layers during training (indicated by gray nodes) while maintaining full network connectivity across all layers. During inference, all neurons are reactivated with no dropout applied. In contrast, our proposed synaptic pruning method permanently removes specific synaptic connections (indicated by red lines) during training, creating a progressively sparser network topology from across all layers.

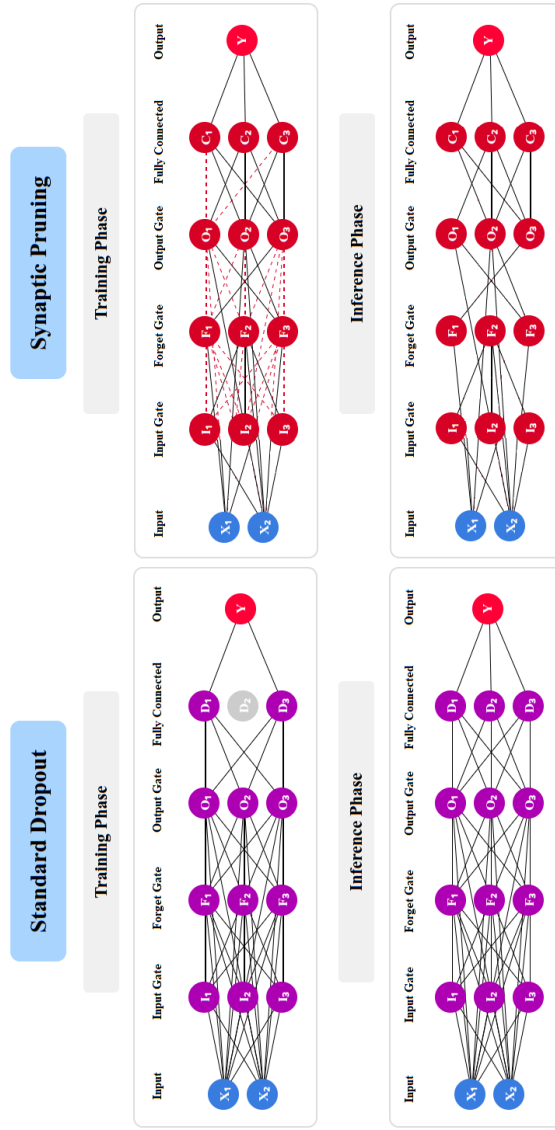


Figure 1: Comparison of standard dropout and our synaptic pruning method implemented on LSTM model architectures. Dropout temporarily deactivates neurons during training, whereas pruning permanently removes specific connections, resulting in lasting sparsity and improved efficiency.

The transformer-based PatchTST implementation (Figure 2) demonstrates similar principles but applies synaptic pruning from the patch to fully con-

nected layers while standard dropout temporarily deactivates nodes within the fully connected layer (indicated by gray nodes).

Across both architectures, solid circles represent active neurons, light gray circles represent temporarily inactive neurons (dropout only), black lines indicate active connections, and red lines highlight pruned connections that remain permanently severed. The key distinction is that dropout provides temporary stochastic regularization without structural modification, while our proposed method creates permanent architectural sparsity that persists through inference, resulting in improved computational efficiency and reduced model complexity while maintaining performance.

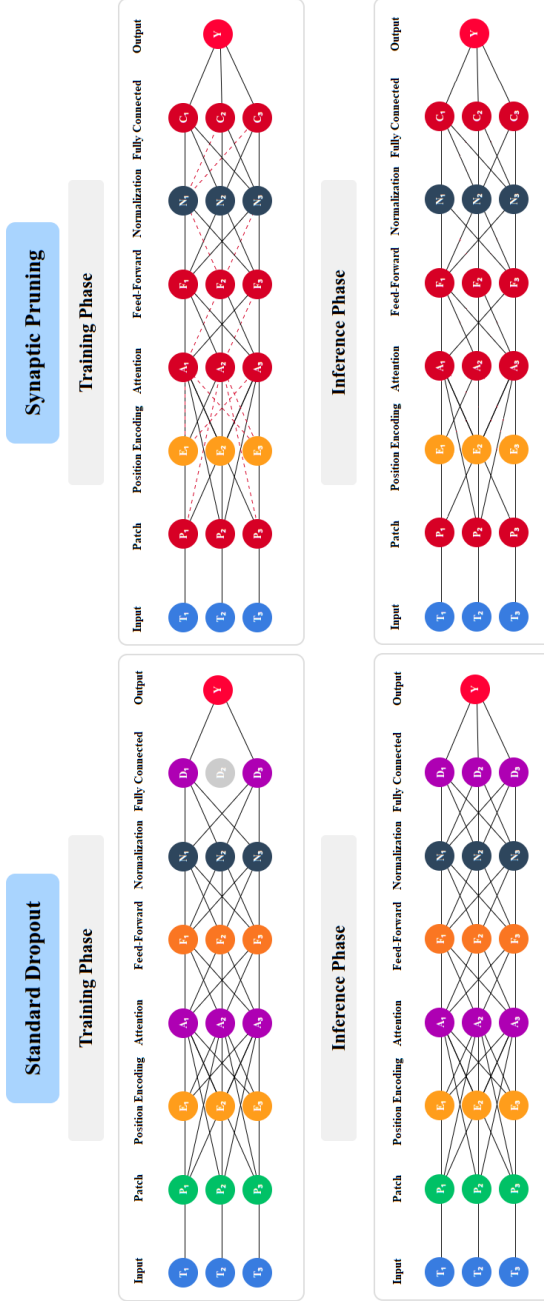


Figure 2: Comparison of standard dropout and our synaptic pruning method implemented on PatchTST model architectures. Dropout temporarily deactivates neurons during training, whereas pruning permanently removes specific connections, resulting in lasting sparsity and improved efficiency.

### 3.7. Datasets

This study employed four diverse public time-series datasets (Table 1) to evaluate the proposed methodology across different domains and complexity levels. The datasets span various application areas including financial markets, cryptocurrency, energy consumption, and environmental monitoring, providing a comprehensive testbed for validation.

Two financial datasets were incorporated: a single stock ticker from the S&P 500 Stocks dataset [23] containing 1,259 records with 20 features, and the Bitcoin Daily historical dataset [24] with 365 records and 7 features. Both financial datasets are classified as low complexity, representing well-structured time series data with established patterns typical of financial markets.

The Household Electric Power Consumption dataset [25] provides the largest sample size with over 2 million records (2,075,259) and 9 features, offering extensive temporal data for energy usage analysis. Despite its substantial size, it maintains low complexity due to the straightforward nature of power consumption measurements.

Finally, the Air Quality dataset [26] presents a moderate-sized dataset with 9,446 records but the highest feature dimensionality at 313 features, resulting in high complexity. This dataset challenges our proposed methodology with high-dimensional environmental data encompassing multiple pollutants and atmospheric conditions. The diversity in dataset characteristics, ranging from 365 to over 2 million records, 7 to 313 features, and varying complexity levels, ensures robust evaluation of the proposed method across different data scenarios and computational challenges.

Table 1: Datasets utilized in this study.

Dataset	Record Count	Features	Complexity
S&P 500 Stocks [23]	1259	20	Low
Bitcoin Daily [24]	365	7	Low
Household Electric Power Consumption [25]	2075259	9	Low
Air Quality [26]	9446	313	High

### 3.8. Experimentation

A total of 96 experiments were performed using RNN, LSTM, and PatchTST architectures, measuring Mean Absolute Error (MAE) when using no regu-

larization, standard dropout, Monte Carlo dropout [27] and our proposed pruning method, using input sequence lengths of 1, 3, 7, 14, 30 and 60. Each experiment was run for 10 trials using varying random seed initialization across a maximum of 20 epochs per trial, with the means of MAE and 95% Confidence Interval (CI) calculated across trials. Experimentation was performed using an Intel i9 20-core CPU and a single Nvidia RTX2080ti GPU. The Python programming language version 3.13.2 with PyTorch version 2.6 was used for all experimentation, with the full source code and utilized data publicly hosted at <https://github.com/xalentis/SynapticPruning>.

## 4. Results and Discussion

Appendix A contains the full results of the 96 experiments. The provided source code includes all experimentation, feature-engineering functions and results analysis modules.

### 4.1. Application to Recurrent Neural Networks (RNN)

The RNN experimental results (Table 2 and Figure 3) confirms that our proposed pruning method consistently outperforms Monte Carlo Dropout across all datasets, with statistically significant improvements in MAE ( $p < 0.05$ ). Compared to standard Dropout, Synaptic Pruning delivers significant gains for the Bitcoin Daily, S&P 500, and Air Quality datasets, but shows no significant difference on the Household Electric Power Consumption dataset. When compared to models trained without regularization, our method achieves comparable or better performance, with statistically significant improvements observed for the Bitcoin, Air Quality, and Electricity datasets, but not for the S&P500 dataset. In terms of computational cost, our method incurs an average overhead of approximately 4.4%, which is modest given its consistent performance gains.

Table 2: RNN model experimentation results and statistical significance.

Dataset	Method	Mean MAE	Std Dev	95% CI	Friedman Test	Overall Significance
Bitcoin Daily	No Dropout	0.3296	0.0546	[0.2933, 0.3659]	$\chi^2 = 15.80$	$p = 0.001246^*$
	Dropout	0.2969	0.0443	[0.2504, 0.3434]		
	MC Dropout	0.3119	0.0315	[0.2788, 0.3450]		
	<b>Synaptic Pruning</b>	<b>0.2621</b>	<b>0.0183</b>	<b>[0.2429, 0.2813]</b>		
S&P500	No Dropout	0.0944	0.0156	[0.0780, 0.1108]	$\chi^2 = 16.76$	$p = 0.000792^*$
	Dropout	0.1105	0.0107	[0.0993, 0.1217]		
	<b>MC Dropout</b>	<b>0.1535</b>	<b>0.0082</b>	<b>[0.1449, 0.1621]</b>		
	Synaptic Pruning	0.0944	0.0156	[0.0780, 0.1108]		
Air Quality	No Dropout	0.8298	0.0219	[0.8068, 0.8528]	$\chi^2 = 16.40$	$p = 0.000939^*$
	Dropout	0.7569	0.0356	[0.7195, 0.7943]		
	MC Dropout	0.7992	0.0308	[0.7669, 0.8315]		
	<b>Synaptic Pruning</b>	<b>0.7265</b>	<b>0.0273</b>	<b>[0.6978, 0.7552]</b>		
Household Electric Power Consumption	No Dropout	0.0902	0.0043	[0.0856, 0.0947]	$\chi^2 = 14.69$	$p = 0.002097$
	Dropout	0.0876	0.0046	[0.0828, 0.0924]		
	MC Dropout	0.1108	0.0034	[0.1073, 0.1144]		
	<b>Synaptic Pruning</b>	<b>0.0855</b>	<b>0.0036</b>	<b>[0.0816, 0.0893]</b>		

### RNN Model Performance

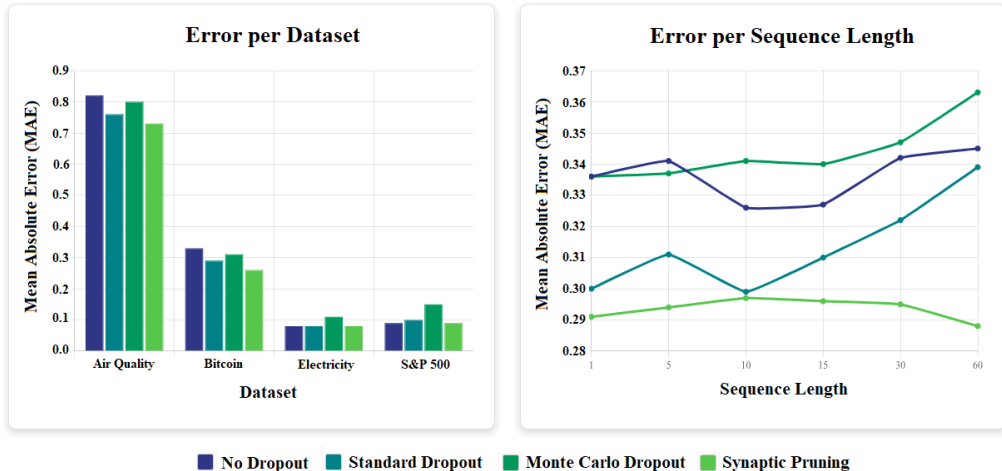


Figure 3: Error rate comparison of regularization methods implemented on RNN model architectures.

#### 4.2. Application to Long Short-Term Memory (LSTM)

LSTM experimental results (Table 3 and Figure 4) reveals that our proposed method achieves an average MAE reduction of 9.8% across all datasets, with performance degradation occurring in 3.3% of cases. Performance gains vary notably by dataset, with the S&P500 dataset exhibiting the largest improvement with a 21.5% average MAE reduction, while the Household Electric Power Consumption dataset shows moderate gains of 8.3%. In contrast, the Bitcoin Daily and Air Quality datasets display marginal improvements of

2.8% and 2.4%, respectively, with limited statistical significance. These findings suggest that while the method's effectiveness can vary depending on the dataset characteristics, it consistently offers meaningful improvements in optimal scenarios with minimal risk of adverse impact, supporting its general applicability for time series forecasting tasks using LSTM models.

Table 3: Long Short-Term Memory experimentation results.

Dataset	Method	Mean MAE	Std Dev	95% CI	Friedman Test	Overall Significance
Bitcoin Daily	No Dropout	0.4804	0.1332	[0.3406, 0.6202]	$\chi^2 = 12.80$	$p = 0.005090$
	Dropout	0.4666	0.1281	[0.3321, 0.6010]		
	MC Dropout	0.4629	0.1208	[0.3361, 0.5897]		
	<b>Synaptic Pruning</b>	<b>0.4212</b>	<b>0.1083</b>	<b>[0.3076, 0.5348]</b>		
S&P500	No Dropout	0.4629	0.0914	[0.3670, 0.5589]	$\chi^2 = 15.40$	$p = 0.001505$
	Dropout	0.5060	0.0703	[0.4322, 0.5798]		
	MC Dropout	0.5102	0.0692	[0.4376, 0.5828]		
	<b>Synaptic Pruning</b>	<b>0.4626</b>	<b>0.0915</b>	<b>[0.3667, 0.5586]</b>		
Air Quality	No Dropout	0.8634	0.0394	[0.8220, 0.9048]	$\chi^2 = 15.20$	$p = 0.001653$
	Dropout	0.8030	0.0415	[0.7595, 0.8466]		
	MC Dropout	0.8431	0.0408	[0.8002, 0.8859]		
	<b>Synaptic Pruning</b>	<b>0.8107</b>	<b>0.0409</b>	<b>[0.7677, 0.8537]</b>		
Household Electric Power Consumption	No Dropout	0.0814	0.0022	[0.0791, 0.0836]	$\chi^2 = 11.60$	$p = 0.008887$
	Dropout	0.0813	0.0015	[0.0797, 0.0829]		
	MC Dropout	0.1046	0.0011	[0.1035, 0.1058]		
	<b>Synaptic Pruning</b>	<b>0.0808</b>	<b>0.0022</b>	<b>[0.0784, 0.0831]</b>		

### LSTM Model Performance

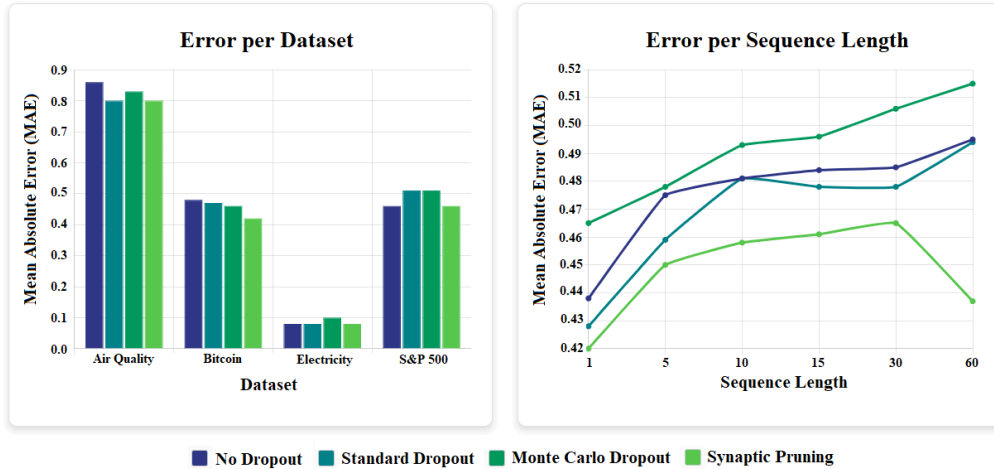


Figure 4: Error rate comparison of regularization methods implemented on LSTM model architectures.

### 4.3. Application to Transformer Networks (PatchTST)

Experimental results using the PatchTST architecture (Figure 5, Table 4) shows our proposed method achieving the best average MAE at 0.42, significantly outperforming using no regularization (0.52), dropout (0.55), and Monte Carlo methods (0.56), with our method reducing MAE by 17.5% to 24.1%. Our proposed method shows statistically significant improvements in 62.5% of experiments, with no cases where it performs significantly worse than alternative methods, and 37.5% showing no significant difference. Performance of our method varies by dataset, with Bitcoin Daily showing exceptional results at 32.0% improvement over other methods, while on the SP&500 dataset demonstrates more modest gains of 10.3% improvement.

Longer sequence lengths benefit more from our pruning method, with 60-step sequences showing 22.0% improvement to 30-step sequences which demonstrate 16.7% improvement. Our proposed method did not perform worse than competing methods across any configuration, potentially establishing it as a reliable regularization technique that consistently maintains or improves model performance.

Table 4: PatchTST experimentation results.

Dataset	Method	Mean MAE	Std MAE	Friedman Test	Rank	Best Pairwise Comparisons (p-value)
Bitcoin	No Dropout	0.3710	0.1481	p=0.000939*	2	vs Dropout (p=0.0312*), vs MC Dropout (p=0.0312*)
	Dropout	0.7740	0.1413		4	Significantly worse than all others
	MC Dropout	0.4620	0.1175		3	vs Dropout (p=0.0312*), vs Synaptic (p=0.0312*)
	<b>Synaptic Pruning</b>	<b>0.3692</b>	0.1460		1	<b>Best performer</b>
S&P500	No Dropout	0.3952	0.1086	p=0.003071*	3	vs MC Dropout (p=0.0312*)
	<b>Dropout</b>	<b>0.3312</b>	0.0685		1	vs MC Dropout (p=0.0312*)
	MC Dropout	0.5923	0.0604		4	Significantly worse than No Dropout and Dropout
	Synaptic Pruning	0.3123	0.0538		2	vs MC Dropout (p=0.0312*)
Air Quality	No Dropout	17.6980	2.4818	p=0.003847*	3	vs Dropout (p=0.0312*)
	Dropout	23.4991	2.7051		4	Significantly worse than MC Dropout and Synaptic
	<b>MC Dropout</b>	<b>16.4987</b>	0.9511		1	vs Dropout (p=0.0312*)
	Synaptic Pruning	16.8684	2.2254		2	vs Dropout (p=0.0312*)
Household Electric Power Consumption	<b>No Dropout</b>	<b>0.1102</b>	0.0093	p=0.000440*	2	vs Dropout (p=0.0312*), vs MC Dropout (p=0.0312*)
	Dropout	0.3114	0.0208		4	Significantly worse than all others
	MC Dropout	0.1316	0.0067		3	vs Dropout (p=0.0312*), vs Synaptic (p=0.0312*)
	<b>Synaptic Pruning</b>	<b>0.1060</b>	0.0083		1	<b>Best performer</b>

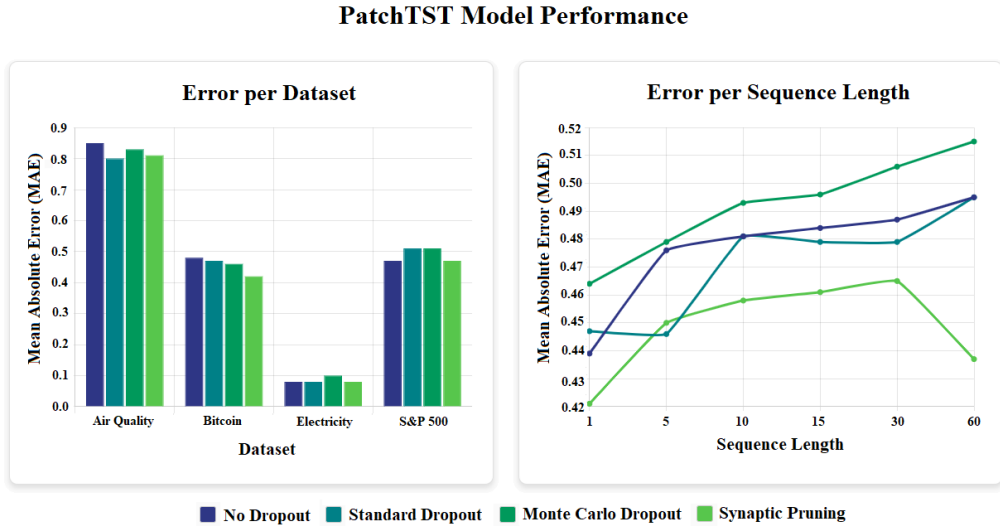


Figure 5: Error rate comparison of regularization methods implemented on PatchTST model architectures.

#### 4.4. Computational Efficiency and Network Sparsification

The proposed synaptic pruning method demonstrates a positive trade-off between computational efficiency and performance across varying sequence lengths. The runtime performance comparison (Figure 6) reveals that while synaptic pruning initially exhibits higher computational overhead at short sequences, it achieves efficiency gains at longer sequences. At sequence length 7, synaptic pruning reaches its optimal performance, significantly outperforming both standard dropout and Monte Carlo dropout (which shows gradual degradation). However, the method exhibits a characteristic U-shaped performance curve, with runtime increasing substantially for very long sequences, though still maintaining competitive performance compared to the baseline without dropout.

The memory usage analysis (Figure 7) provides insights into the method’s scalability characteristics. All approaches demonstrate similar memory consumption patterns, with peak usage stabilizing after sequence length 3. This memory consistency across different sequence lengths suggests that the pruning mechanism effectively manages computational resources without introducing significant memory overhead.

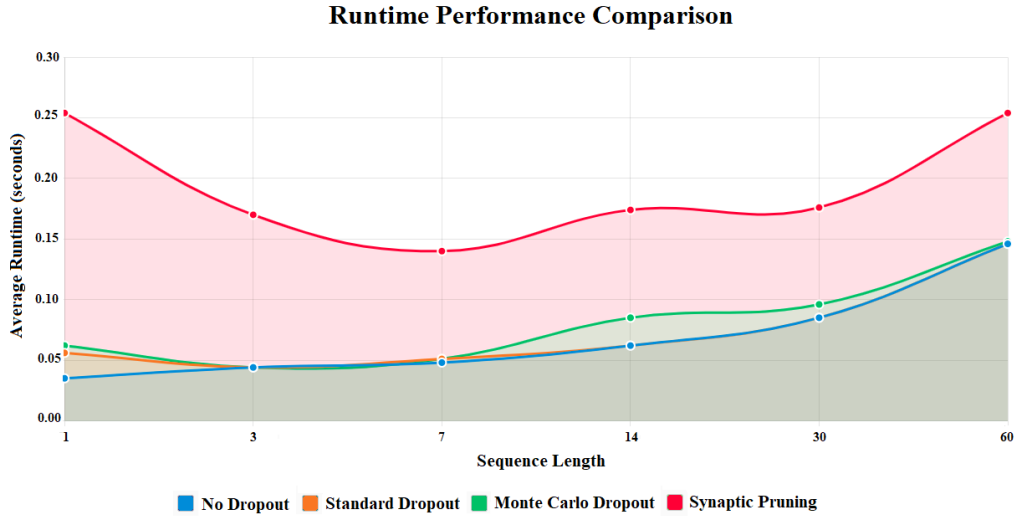


Figure 6: Average pruning sparsity rates by model.

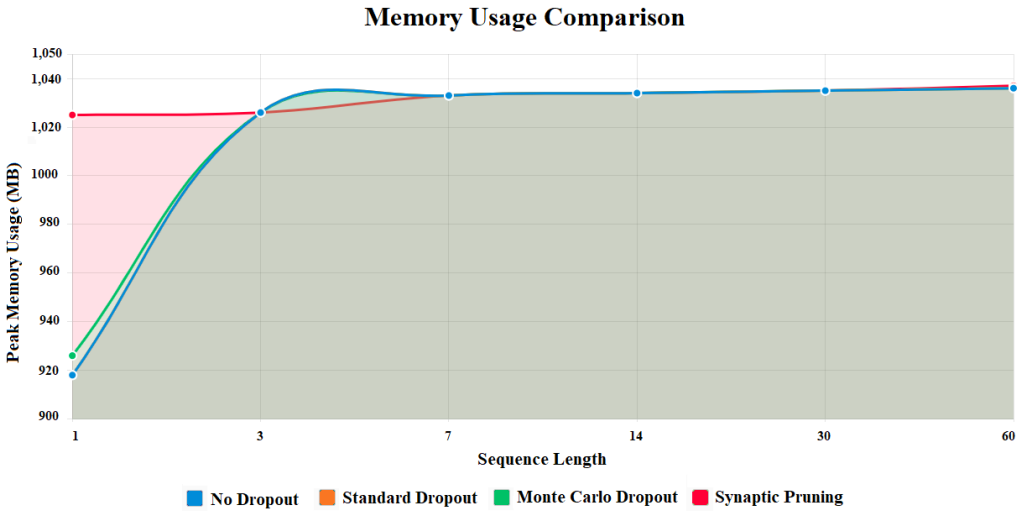


Figure 7: Average memory reduction rates by model.

#### 4.5. Biological Plausibility and Neuro-scientific Validation

Our proposed method's biological inspiration extends beyond superficial analogies to incorporate quantifiable aspects of synaptic pruning mechanisms, mir-

roring activity-dependent synaptic strengthening observed in long-term potentiation (LTP) [28] and long-term depression (LTD) [29]. The temporal dynamics of our pruning process align with developmental timescales observed in cortical maturation [30]. This biological grounding distinguishes our approach from purely engineering-based pruning methods and suggests potential for further bio-inspired enhancements.

Performance results reveal that synaptic pruning is particularly well-suited for moderate sequence lengths (3-14), where it achieves optimal efficiency. This behavior pattern aligns with the adaptive nature of biological synaptic pruning, where neural circuits optimize themselves for frequently encountered input patterns. The method’s ability to maintain stable memory usage while providing variable runtime performance could be particularly valuable for applications with diverse sequence length requirements [31, 32]. Our analysis shows that networks converge to optimal sparsity levels within the first 15 epochs, after which the pruning rate stabilizes. This early convergence behavior aligns with biological observations of critical periods of brain development [33, 34], suggesting that our method captures fundamental principles of neural circuit optimization during these developmental windows.

## 5. Study Limitations

While the results from the study indicate potential in the use of a more targeted approach to regularization compared to current dropout approaches, a number of limitations require future work and experimentation. First, a relatively small number of model architectures and network configurations were tested, limiting generalizability to other critical architectures such as vision transformers, and modern large language models. Secondly, experimentation was conducted using CPU or a single GPU system without using parallel data transfer during the pruning phase, which will require additional consideration when experimenting on significantly larger training datasets. The computational overhead observed may compound significantly at enterprise scale, and our limited experimentation may not reflect modern big data scenarios where scalability becomes critical.

## 6. Conclusion and Future Work

This study introduces a biologically-inspired regularization technique that aims to mimic synaptic pruning in the developing brain, offering an alter-

native to current dropout approaches for neural network regularization. By dynamically evaluating neurons based on importance metrics and permanently removing connections with minimal contribution to error reduction, our proposed approach significantly enhances predictive accuracy. The error reduction observed in our PatchTST experiments, when applied to time series forecasting, demonstrates the efficacy of activity-dependent pruning over conventional regularization methods.

The success of our approach aligns with the neuro-scientific understanding of brain development, where synaptic elimination occurs based on functional utility rather than stochastic processes. This bio-mimetic strategy preserves critical pathways while removing redundant connections, resulting in sparser networks with improved generalization capabilities.

Future work should address the computational overhead through optimized implementation and parallelization techniques with validation on larger datasets. Long-term research directions should explore implementations that include both synaptic growth and pruning phases, potentially leading to next-generation bio-inspired architectures that fundamentally change how neural networks learn and adapt. By continuing to incorporate neuro-biological principles into deep learning, we envision improved and novel techniques that enable neural networks to better emulate the remarkable efficiency and generalization capabilities of biological learning systems.

## 7. Supplementary Material: Appendix A

## RNN Model Results

Dataset	Model	Metric	Sequence Length	No Dropout	Dropout	MC Dropout	Synaptic Pruning
Bitcoin	RNN	mae	1	0.3236	0.3152	0.3176	0.2900
Bitcoin	RNN	runtime	1	0.3705	0.3623	0.3737	0.3388
Bitcoin	RNN	mae_95ci_low	1	0.2491	0.2370	0.2330	0.2380
Bitcoin	RNN	mae_95ci_high	1	0.3981	0.3934	0.4023	0.3421
Bitcoin	RNN	mae	3	0.3113	0.2679	0.2969	0.2455
Bitcoin	RNN	runtime	3	0.3591	0.3167	0.3563	0.3047
Bitcoin	RNN	mae_95ci_low	3	0.2451	0.2043	0.2313	0.2117
Bitcoin	RNN	mae_95ci_high	3	0.3774	0.3314	0.3626	0.2794
Bitcoin	RNN	mae	7	0.3006	0.2564	0.2860	0.2681
Bitcoin	RNN	rmse	7	0.3466	0.3054	0.3434	0.3360
Bitcoin	RNN	mae_95ci_low	7	0.2118	0.1733	0.2039	0.1690
Bitcoin	RNN	mae_95ci_high	7	0.3894	0.3395	0.3680	0.3672
Bitcoin	RNN	mae	14	0.3180	0.2703	0.2864	0.2699
Bitcoin	RNN	rmse	14	0.3638	0.3175	0.3469	0.3189
Bitcoin	RNN	mae_95ci_low	14	0.2391	0.1928	0.2052	0.2166
Bitcoin	RNN	mae_95ci_high	14	0.3969	0.3478	0.3676	0.3232
Bitcoin	RNN	mae	30	0.3263	0.2954	0.3144	0.2395
Bitcoin	RNN	rmse	30	0.3695	0.3403	0.3698	0.2934
Bitcoin	RNN	mae_95ci_low	30	0.2699	0.2158	0.2269	0.1787
Bitcoin	RNN	mae_95ci_high	30	0.3826	0.3750	0.4018	0.3002
Bitcoin	RNN	mae	60	0.3976	0.3763	0.3701	0.2596
Bitcoin	RNN	runtime	60	0.4381	0.4175	0.4205	0.3117
Bitcoin	RNN	mae_95ci_low	60	0.2694	0.2536	0.2296	0.1040
Bitcoin	RNN	mae_95ci_high	60	0.5257	0.4990	0.5105	0.4152
S&P500	RNN	mae	1	0.1062	0.1096	0.1668	0.1060
S&P500	RNN	rmse	1	0.1449	0.1434	0.2182	0.1447
S&P500	RNN	mae_95ci_low	1	0.0955	0.0947	0.1525	0.0952
S&P500	RNN	mae_95ci_high	1	0.1170	0.1245	0.1811	0.1168
S&P500	RNN	mae	3	0.1204	0.1285	0.1571	0.1205
S&P500	RNN	rmse	3	0.1595	0.1655	0.2061	0.1596
S&P500	RNN	mae_95ci_low	3	0.0941	0.0995	0.1364	0.0940
S&P500	RNN	mae_95ci_high	3	0.1468	0.1576	0.1778	0.1470

S&P500	RNN	mae	7	0.0792	0.0951	0.1437	0.0792
S&P500	RNN	rmse	7	0.1095	0.1254	0.1880	0.1095
S&P500	RNN	mae_95ci_low	7	0.0631	0.0766	0.1297	0.0628
S&P500	RNN	mae_95ci_high	7	0.0954	0.1136	0.1576	0.0955
S&P500	RNN	mae	14	0.0845	0.1082	0.1500	0.0845
S&P500	RNN	rmse	14	0.1147	0.1372	0.1953	0.1148
S&P500	RNN	mae_95ci_low	14	0.0636	0.0646	0.1300	0.0638
S&P500	RNN	mae_95ci_high	14	0.1053	0.1517	0.1701	0.1053
S&P500	RNN	mae	30	0.0879	0.1104	0.1478	0.0878
S&P500	RNN	rmse	30	0.1184	0.1410	0.1928	0.1184
S&P500	RNN	mae_95ci_low	30	0.0679	0.0835	0.1290	0.0679
S&P500	RNN	mae_95ci_high	30	0.1079	0.1373	0.1666	0.1078
S&P500	RNN	mae	60	0.0883	0.1113	0.1558	0.0884
S&P500	RNN	rmse	60	0.1182	0.1414	0.2024	0.1184
S&P500	RNN	mae_95ci_low	60	0.0669	0.0815	0.1310	0.0670
S&P500	RNN	mae_95ci_high	60	0.1097	0.1412	0.1807	0.1098
Air Quality	RNN	mae	1	0.8347	0.6915	0.7412	0.6881
Air Quality	RNN	rmse	1	1.0609	0.9188	0.9691	0.9360
Air Quality	RNN	mae_95ci_low	1	0.8123	0.6746	0.7323	0.6723
Air Quality	RNN	mae_95ci_high	1	0.8570	0.7084	0.7501	0.7039
Air Quality	RNN	mae	3	0.8404	0.7604	0.7875	0.7087
Air Quality	RNN	rmse	3	1.0879	0.9909	1.0193	0.9513
Air Quality	RNN	mae_95ci_low	3	0.7925	0.7190	0.7583	0.6863
Air Quality	RNN	mae_95ci_high	3	0.8883	0.8018	0.8168	0.7311
Air Quality	RNN	mae	7	0.8287	0.7498	0.8190	0.7337
Air Quality	RNN	rmse	7	1.0739	0.9904	1.0595	0.9621
Air Quality	RNN	mae_95ci_low	7	0.7820	0.7334	0.7832	0.6999
Air Quality	RNN	mae_95ci_high	7	0.8754	0.7663	0.8548	0.7674
Air Quality	RNN	mae	14	0.8128	0.7715	0.8137	0.7440
Air Quality	RNN	rmse	14	1.0479	1.0050	1.0496	0.9772
Air Quality	RNN	mae_95ci_low	14	0.7637	0.7429	0.7844	0.6950
Air Quality	RNN	mae_95ci_high	14	0.8619	0.8000	0.8429	0.7930
Air Quality	RNN	mae	30	0.8625	0.7968	0.8138	0.7655
Air Quality	RNN	rmse	30	1.1118	1.0278	1.0515	0.9994
Air Quality	RNN	mae_95ci_low	30	0.8098	0.7505	0.7740	0.6988
Air Quality	RNN	mae_95ci_high	30	0.9152	0.8430	0.8537	0.8321

Air Quality	RNN	mae	60	0.7996	0.7713	0.8200	0.7190
Air Quality	RNN	rmse	60	1.0317	1.0042	1.0541	0.9550
Air Quality	RNN	mae_95ci_low	60	0.7536	0.7331	0.7921	0.6860
Air Quality	RNN	mae_95ci_high	60	0.8456	0.8095	0.8478	0.7520
Electricity	RNN	mae	1	0.0817	0.0806	0.1043	0.0814
Electricity	RNN	rmse	1	0.1980	0.1998	0.2125	0.1982
Electricity	RNN	mae_95ci_low	1	0.0793	0.0767	0.1019	0.0783
Electricity	RNN	mae_95ci_high	1	0.0840	0.0845	0.1067	0.0845
Electricity	RNN	mae	3	0.0928	0.0886	0.1116	0.0899
Electricity	RNN	rmse	3	0.2018	0.2022	0.2172	0.2005
Electricity	RNN	mae_95ci_low	3	0.0864	0.0817	0.1075	0.0823
Electricity	RNN	mae_95ci_high	3	0.0992	0.0954	0.1158	0.0974
Electricity	RNN	mae	7	0.0922	0.0922	0.1143	0.0900
Electricity	RNN	rmse	7	0.2019	0.2025	0.2194	0.2000
Electricity	RNN	mae_95ci_low	7	0.0861	0.0786	0.1103	0.0840
Electricity	RNN	mae_95ci_high	7	0.0982	0.1058	0.1183	0.0960
Electricity	RNN	mae	14	0.0932	0.0887	0.1117	0.0845
Electricity	RNN	rmse	14	0.1995	0.2026	0.2176	0.1970
Electricity	RNN	mae_95ci_low	14	0.0862	0.0833	0.1088	0.0792
Electricity	RNN	mae_95ci_high	14	0.1002	0.0941	0.1147	0.0898
Electricity	RNN	mae	30	0.0915	0.0838	0.1122	0.0830
Electricity	RNN	rmse	30	0.1966	0.1986	0.2184	0.1934
Electricity	RNN	mae_95ci_low	30	0.0857	0.0795	0.1083	0.0792
Electricity	RNN	mae_95ci_high	30	0.0972	0.0881	0.1161	0.0868
Electricity	RNN	mae	60	0.0895	0.0919	0.1109	0.0839
Electricity	RNN	rmse	60	0.1958	0.2005	0.2159	0.1940
Electricity	RNN	mae_95ci_low	60	0.0856	0.0843	0.1066	0.0806
Electricity	RNN	mae_95ci_high	60	0.0933	0.0995	0.1153	0.0872

## LSTM Model Results

Dataset	Model	Metric	Sequence Length	No Dropout	Dropout	MC Dropout	Synaptic Pruning
Bitcoin	LSTM	mae	1	0.2447	0.2444	0.2551	0.2359
Bitcoin	LSTM	runtime	1	0.1190	0.1079	0.1176	1.8706
Bitcoin	LSTM	mae_95ci_low	1	0.2343	0.2346	0.2438	0.2249
Bitcoin	LSTM	mae_95ci_high	1	0.2551	0.2542	0.2664	0.2468
Bitcoin	LSTM	mae	3	0.4187	0.4072	0.4104	0.3513
Bitcoin	LSTM	runtime	3	0.0674	0.0697	0.0725	1.0815
Bitcoin	LSTM	mae_95ci_low	3	0.3914	0.3813	0.3832	0.3339
Bitcoin	LSTM	mae_95ci_high	3	0.4460	0.4330	0.4376	0.3686
Bitcoin	LSTM	mae	7	0.4992	0.4756	0.4832	0.4522
Bitcoin	LSTM	runtime	7	0.0713	0.0720	0.0808	0.8494
Bitcoin	LSTM	mae_95ci_low	7	0.4273	0.4074	0.4082	0.4250
Bitcoin	LSTM	mae_95ci_high	7	0.5711	0.5437	0.5582	0.4794
Bitcoin	LSTM	mae	14	0.5430	0.5197	0.4818	0.4914
Bitcoin	LSTM	runtime	14	0.0704	0.0717	0.1031	0.9094
Bitcoin	LSTM	mae_95ci_low	14	0.4722	0.4473	0.3992	0.4431
Bitcoin	LSTM	mae_95ci_high	14	0.6138	0.5922	0.5645	0.5398
Bitcoin	LSTM	mae	30	0.5586	0.5430	0.5425	0.5265
Bitcoin	LSTM	runtime	30	0.0666	0.0721	0.0772	0.7618
Bitcoin	LSTM	mae_95ci_low	30	0.4872	0.4715	0.4639	0.4842
Bitcoin	LSTM	mae_95ci_high	30	0.6301	0.6146	0.6210	0.5688
Bitcoin	LSTM	mae	60	0.6182	0.6096	0.6042	0.4701
Bitcoin	LSTM	rmse	60	0.6526	0.6443	0.6499	0.5116
Bitcoin	LSTM	mae_95ci_low	60	0.5826	0.5792	0.5737	0.4454
Bitcoin	LSTM	mae_95ci_high	60	0.6537	0.6400	0.6347	0.4949
S&P500	LSTM	mae	1	0.6263	0.6384	0.6374	0.6260
S&P500	LSTM	runtime	1	0.5891	0.6019	0.6050	1.3054
S&P500	LSTM	mae_95ci_low	1	0.5950	0.6119	0.6122	0.5945
S&P500	LSTM	mae_95ci_high	1	0.6576	0.6649	0.6625	0.6575
S&P500	LSTM	mae	3	0.5063	0.5251	0.5272	0.5061
S&P500	LSTM	runtime	3	0.6354	0.6515	0.6580	1.3512
S&P500	LSTM	mae_95ci_low	3	0.4747	0.5022	0.5017	0.4737
S&P500	LSTM	mae_95ci_high	3	0.5379	0.5480	0.5526	0.5386

S&P500	LSTM	mae	7	0.4444	0.4815	0.4966	0.4445
S&P500	LSTM	runtime	7	0.7500	0.7645	0.7568	1.4485
S&P500	LSTM	mae_95ci_low	7	0.4071	0.4512	0.4571	0.4064
S&P500	LSTM	mae_95ci_high	7	0.4818	0.5117	0.5360	0.4826
S&P500	LSTM	mae	14	0.4249	0.4845	0.4943	0.4242
S&P500	LSTM	runtime	14	0.8765	0.8859	0.9057	1.5774
S&P500	LSTM	mae_95ci_low	14	0.3822	0.4492	0.4682	0.3806
S&P500	LSTM	mae_95ci_high	14	0.4675	0.5199	0.5204	0.4678
S&P500	LSTM	mae	30	0.3963	0.4631	0.4675	0.3960
S&P500	LSTM	runtime	30	1.1833	1.1958	1.1878	1.8796
S&P500	LSTM	mae_95ci_low	30	0.3557	0.4289	0.4268	0.3553
S&P500	LSTM	mae_95ci_high	30	0.4368	0.4972	0.5081	0.4367
S&P500	LSTM	mae	60	0.3794	0.4434	0.4381	0.3790
S&P500	LSTM	runtime	60	1.7871	1.8529	1.8439	2.4188
S&P500	LSTM	mae_95ci_low	60	0.3411	0.4067	0.4049	0.3398
S&P500	LSTM	mae_95ci_high	60	0.4177	0.4801	0.4713	0.4181
Air Quality	LSTM	mae	1	0.8058	0.7439	0.7832	0.7418
Air Quality	LSTM	rmse	1	1.0676	0.9933	1.0397	0.9920
Air Quality	LSTM	mae_95ci_low	1	0.7660	0.7327	0.7550	0.7214
Air Quality	LSTM	mae_95ci_high	1	0.8455	0.7551	0.8114	0.7621
Air Quality	LSTM	mae	3	0.8256	0.7639	0.8111	0.7861
Air Quality	LSTM	rmse	3	1.1091	1.0337	1.0868	1.0505
Air Quality	LSTM	mae_95ci_low	3	0.7956	0.7341	0.7922	0.7521
Air Quality	LSTM	mae_95ci_high	3	0.8557	0.7938	0.8300	0.8200
Air Quality	LSTM	mae	7	0.8735	0.7990	0.8336	0.8196
Air Quality	LSTM	rmse	7	1.1638	1.0892	1.1136	1.1028
Air Quality	LSTM	mae_95ci_low	7	0.8309	0.7738	0.8096	0.7958
Air Quality	LSTM	mae_95ci_high	7	0.9161	0.8243	0.8576	0.8433
Air Quality	LSTM	mae	14	0.8742	0.8393	0.8831	0.8372
Air Quality	LSTM	rmse	14	1.1560	1.1304	1.1704	1.1089
Air Quality	LSTM	mae_95ci_low	14	0.8292	0.8192	0.8427	0.8030
Air Quality	LSTM	mae_95ci_high	14	0.9192	0.8595	0.9235	0.8714
Air Quality	LSTM	mae	30	0.9045	0.8298	0.8651	0.8565
Air Quality	LSTM	runtime	30	6.3374	6.7021	9.1254	26.6938
Air Quality	LSTM	mae_95ci_low	30	0.8668	0.8058	0.8286	0.8219
Air Quality	LSTM	mae_95ci_high	30	0.9423	0.8539	0.9017	0.8911

Air Quality	LSTM	mae	60	0.8968	0.8422	0.8824	0.8230
Air Quality	LSTM	runtime	60	22.9802	24.6852	20.3635	54.5859
Air Quality	LSTM	mae_95ci_low	60	0.8677	0.8131	0.8575	0.7680
Air Quality	LSTM	mae_95ci_high	60	0.9258	0.8712	0.9072	0.8780
Electricity	LSTM	mae	1	0.0792	0.0824	0.1038	0.0782
Electricity	LSTM	runtime	1	7.8921	7.8495	7.8987	95.7385
Electricity	LSTM	mae_95ci_low	1	0.0765	0.0791	0.1020	0.0755
Electricity	LSTM	mae_95ci_high	1	0.0818	0.0857	0.1056	0.0809
Electricity	LSTM	mae	3	0.0826	0.0817	0.1049	0.0800
Electricity	LSTM	runtime	3	7.7053	8.5866	8.8290	88.8553
Electricity	LSTM	mae_95ci_low	3	0.0773	0.0761	0.1020	0.0756
Electricity	LSTM	mae_95ci_high	3	0.0880	0.0873	0.1078	0.0844
Electricity	LSTM	mae	7	0.0812	0.0809	0.1045	0.0795
Electricity	LSTM	runtime	7	8.5592	9.3183	9.5516	102.5181
Electricity	LSTM	mae_95ci_low	7	0.0768	0.0791	0.1030	0.0758
Electricity	LSTM	mae_95ci_high	7	0.0856	0.0826	0.1059	0.0832
Electricity	LSTM	mae	14	0.0814	0.0832	0.1060	0.0822
Electricity	LSTM	runtime	14	9.3840	9.0948	9.2311	97.2820
Electricity	LSTM	mae_95ci_low	14	0.0777	0.0774	0.1045	0.0776
Electricity	LSTM	mae_95ci_high	14	0.0852	0.0890	0.1076	0.0867
Electricity	LSTM	mae	30	0.0848	0.0806	0.1056	0.0844
Electricity	LSTM	runtime	30	8.4287	10.1354	9.7164	99.5264
Electricity	LSTM	mae_95ci_low	30	0.0814	0.0776	0.1033	0.0804
Electricity	LSTM	mae_95ci_high	30	0.0883	0.0836	0.1080	0.0885
Electricity	LSTM	mae	60	0.0791	0.0789	0.1031	0.0802
Electricity	LSTM	runtime	60	9.9183	9.6104	10.2516	104.8715
Electricity	LSTM	mae_95ci_low	60	0.0770	0.0757	0.1017	0.0758
Electricity	LSTM	mae_95ci_high	60	0.0812	0.0822	0.1046	0.0846

## PatchTST Model Results

Dataset	Model	Metric	Sequence Length	No Dropout	Dropout	MC Dropout	Synaptic Pruning
Bitcoin	PatchTST	mae	1	0.1821	0.7143	0.4325	0.1916
Bitcoin	PatchTST	runtime	1	0.2219	0.7396	0.5080	0.2309
Bitcoin	PatchTST	mae_95ci_low	1	0.1418	0.6519	0.3574	0.1425
Bitcoin	PatchTST	mae_95ci_high	1	0.2225	0.7768	0.5075	0.2407
Bitcoin	PatchTST	mae	3	0.3130	0.6621	0.3317	0.3131
Bitcoin	PatchTST	runtime	3	0.3524	0.6877	0.3915	0.3524
Bitcoin	PatchTST	mae_95ci_low	3	0.1950	0.5242	0.2391	0.1954
Bitcoin	PatchTST	mae_95ci_high	3	0.4311	0.7999	0.4244	0.4307
Bitcoin	PatchTST	mae	7	0.2952	0.6561	0.3696	0.2810
Bitcoin	PatchTST	rmse	7	0.3434	0.6856	0.4277	0.3281
Bitcoin	PatchTST	mae_95ci_low	7	0.1890	0.5071	0.2686	0.1690
Bitcoin	PatchTST	mae_95ci_high	7	0.4013	0.8051	0.4705	0.3931
Bitcoin	PatchTST	mae	14	0.3173	0.6680	0.4041	0.3172
Bitcoin	PatchTST	rmse	14	0.3678	0.7005	0.4652	0.3677
Bitcoin	PatchTST	mae_95ci_low	14	0.2265	0.5547	0.3038	0.2263
Bitcoin	PatchTST	mae_95ci_high	14	0.4081	0.7813	0.5044	0.4082
Bitcoin	PatchTST	mae	30	0.4780	0.9609	0.5666	0.4761
Bitcoin	PatchTST	rmse	30	0.5245	0.9904	0.6186	0.5228
Bitcoin	PatchTST	mae_95ci_low	30	0.3573	0.8008	0.4461	0.3530
Bitcoin	PatchTST	mae_95ci_high	30	0.5987	1.1210	0.6871	0.5992
Bitcoin	PatchTST	mae	60	0.6402	0.9828	0.6674	0.6362
Bitcoin	PatchTST	runtime	60	0.6797	1.0121	0.7097	0.6759
Bitcoin	PatchTST	mae_95ci_low	60	0.5903	0.9323	0.6275	0.5902
Bitcoin	PatchTST	mae_95ci_high	60	0.6901	1.0334	0.7073	0.6821
S&P500	PatchTST	mae	1	0.2819	0.4299	0.6804	0.2838
S&P500	PatchTST	rmse	1	0.3408	0.5177	0.7712	0.3760
S&P500	PatchTST	mae_95ci_low	1	0.2403	0.3876	0.6483	0.2711
S&P500	PatchTST	mae_95ci_high	1	0.3236	0.4721	0.7124	0.3643
S&P500	PatchTST	mae	3	0.3008	0.2797	0.5755	0.2925
S&P500	PatchTST	rmse	3	0.3584	0.3624	0.6553	0.3514
S&P500	PatchTST	mae_95ci_low	3	0.2641	0.2563	0.5336	0.2548
S&P500	PatchTST	mae_95ci_high	3	0.3374	0.3030	0.6174	0.3301

S&P500	PatchTST	mae	7	0.3180	0.2358	0.5145	0.2358
S&P500	PatchTST	rmse	7	0.3772	0.3023	0.5892	0.3024
S&P500	PatchTST	mae_95ci_low	7	0.2745	0.1998	0.4767	0.1999
S&P500	PatchTST	mae_95ci_high	7	0.3614	0.2717	0.5523	0.2717
S&P500	PatchTST	mae	14	0.4077	0.3048	0.5307	0.3121
S&P500	PatchTST	rmse	14	0.4825	0.3918	0.6164	0.4006
S&P500	PatchTST	mae_95ci_low	14	0.3675	0.2780	0.4984	0.2807
S&P500	PatchTST	mae_95ci_high	14	0.4479	0.3315	0.5631	0.3436
S&P500	PatchTST	mae	30	0.4779	0.3286	0.5970	0.3398
S&P500	PatchTST	rmse	30	0.5645	0.4230	0.6886	0.4366
S&P500	PatchTST	mae_95ci_low	30	0.4470	0.2957	0.5514	0.3145
S&P500	PatchTST	mae_95ci_high	30	0.5088	0.3616	0.6426	0.3652
S&P500	PatchTST	mae	60	0.5850	0.4083	0.6555	0.4099
S&P500	PatchTST	rmse	60	0.6708	0.5186	0.7415	0.5208
S&P500	PatchTST	mae_95ci_low	60	0.5320	0.3573	0.6054	0.3602
S&P500	PatchTST	mae_95ci_high	60	0.6380	0.4592	0.7056	0.4595
Air Quality	PatchTST	mae	1	16.1275	27.0567	15.9646	15.6985
Air Quality	PatchTST	rmse	1	45.3082	53.2031	45.4585	45.0086
Air Quality	PatchTST	mae_95ci_low	1	14.8850	25.4175	14.6479	14.1160
Air Quality	PatchTST	mae_95ci_high	1	17.3700	28.6960	17.2813	17.2810
Air Quality	PatchTST	mae	3	19.7196	22.5570	15.2132	19.9416
Air Quality	PatchTST	rmse	3	43.8000	46.8524	42.7943	43.8994
Air Quality	PatchTST	mae_95ci_low	3	13.0623	17.3900	13.7394	12.9484
Air Quality	PatchTST	mae_95ci_high	3	26.3769	27.7240	16.6871	26.9347
Air Quality	PatchTST	mae	7	16.2646	20.0300	15.6466	15.9935
Air Quality	PatchTST	rmse	7	43.0241	45.9279	42.7583	43.0292
Air Quality	PatchTST	mae_95ci_low	7	11.5829	14.2740	12.0707	12.4944
Air Quality	PatchTST	mae_95ci_high	7	20.9463	25.7861	19.2225	19.4926
Air Quality	PatchTST	mae	14	19.3945	21.5496	17.5457	18.3663
Air Quality	PatchTST	rmse	14	43.3334	46.6010	43.2483	43.7783
Air Quality	PatchTST	mae_95ci_low	14	15.3269	15.5848	13.4590	14.2256
Air Quality	PatchTST	mae_95ci_high	14	23.4622	27.5145	21.6323	22.5071
Air Quality	PatchTST	mae	30	13.7902	22.5991	16.8941	13.0852
Air Quality	PatchTST	rmse	30	44.1359	47.5883	43.8919	43.6895
Air Quality	PatchTST	mae_95ci_low	30	11.0907	20.0749	11.4158	11.3914
Air Quality	PatchTST	mae_95ci_high	30	16.4896	25.1234	22.3725	14.7790

Air Quality	PatchTST	mae	60	20.8918	27.2025	17.7279	18.1252
Air Quality	PatchTST	rmse	60	50.0566	54.5919	46.9463	47.3044
Air Quality	PatchTST	mae_95ci_low	60	10.7801	21.5402	15.0372	13.6740
Air Quality	PatchTST	mae_95ci_high	60	31.0035	32.8647	20.4186	22.5763
Electricity	PatchTST	mae	1	0.1009	0.2832	0.1447	0.0989
Electricity	PatchTST	rmse	1	0.1859	0.3637	0.2240	0.1857
Electricity	PatchTST	mae_95ci_low	1	0.0902	0.2655	0.1408	0.0862
Electricity	PatchTST	mae_95ci_high	1	0.1117	0.3009	0.1487	0.1116
Electricity	PatchTST	mae	3	0.1146	0.3411	0.1331	0.1070
Electricity	PatchTST	rmse	3	0.1909	0.4212	0.2121	0.1862
Electricity	PatchTST	mae_95ci_low	3	0.0990	0.3022	0.1248	0.0916
Electricity	PatchTST	mae_95ci_high	3	0.1302	0.3800	0.1414	0.1223
Electricity	PatchTST	mae	7	0.1015	0.3279	0.1265	0.1014
Electricity	PatchTST	rmse	7	0.1822	0.4084	0.2038	0.1825
Electricity	PatchTST	mae_95ci_low	7	0.0893	0.2902	0.1149	0.0894
Electricity	PatchTST	mae_95ci_high	7	0.1137	0.3657	0.1381	0.1134
Electricity	PatchTST	mae	14	0.1011	0.3079	0.1310	0.0952
Electricity	PatchTST	rmse	14	0.1847	0.3856	0.2071	0.1825
Electricity	PatchTST	mae_95ci_low	14	0.0867	0.2902	0.1160	0.0819
Electricity	PatchTST	mae_95ci_high	14	0.1154	0.3256	0.1460	0.1084
Electricity	PatchTST	mae	30	0.1214	0.2879	0.1233	0.1175
Electricity	PatchTST	rmse	30	0.1976	0.3653	0.1993	0.1957
Electricity	PatchTST	mae_95ci_low	30	0.1003	0.2594	0.1149	0.0967
Electricity	PatchTST	mae_95ci_high	30	0.1425	0.3165	0.1317	0.1383
Electricity	PatchTST	mae	60	0.1218	0.3206	0.1312	0.1158
Electricity	PatchTST	rmse	60	0.2049	0.3934	0.2076	0.2018
Electricity	PatchTST	mae_95ci_low	60	0.1057	0.2765	0.1185	0.0990
Electricity	PatchTST	mae_95ci_high	60	0.1379	0.3646	0.1440	0.1325

## References

- [1] P. Rakic, J.-P. Bourgeois, M. F. Eckenhoff, N. Zecevic, P. S. Goldman-Rakic, Overproduction of synapses in diverse regions of the primate cerebral cortex, *Science* 232 (1994) 232–235.
- [2] P. R. Huttenlocher, A. S. Dabholkar, Regional differences in synaptogenesis in human cerebral cortex, *Journal of Comparative Neurology* 387 (2) (1997) 167–178.
- [3] G. Chechik, I. Meilijson, E. Ruppin, Synaptic pruning in development: a computational account, *Neural Computation* 10 (7) (1998) 1759–1777.
- [4] L. D. Selement, P. S. Goldman-Rakic, The reduced neuropil hypothesis: a circuit based model of schizophrenia, *Biological psychiatry* 45 (1) (1999) 17–25.
- [5] Y. Zhan, R. C. Paolicelli, F. Sforazzini, L. Weinhard, G. Bolasco, F. Paganini, A. L. Vyssotski, A. Bifone, A. Gozzi, D. Ragozzino, et al., Deficient neuron-microglia signaling results in impaired functional brain connectivity and social behavior, *Nature neuroscience* 17 (3) (2014) 400–406.
- [6] G. Tang, K. Gudsnuk, S.-H. Kuo, M. L. Cotrina, G. Rosoklja, A. Sosunov, M. S. Sonders, E. Kanter, C. Castagna, A. Yamamoto, et al., Loss of mtor-dependent macroautophagy causes autistic-like synaptic pruning deficits, *Neuron* 83 (5) (2014) 1131–1143.
- [7] Y. LeCun, J. S. Denker, S. A. Solla, Optimal brain damage, in: *Advances in Neural Information Processing Systems*, Vol. 2, 1990, pp. 598–605.
- [8] D. Hassabis, D. Kumaran, C. Summerfield, M. Botvinick, Neuroscience-inspired artificial intelligence, *Neuron* 95 (2) (2017) 245–258. doi:10.1016/j.neuron.2017.06.011.
- [9] S. Han, J. Pool, J. Tran, W. J. Dally, Learning both weights and connections for efficient neural networks, *Advances in neural information processing systems* 28 (2015).
- [10] N. Srivastava, G. Hinton, A. Krizhevsky, I. Sutskever, R. Salakhutdinov, Dropout: A simple way to prevent neural networks from overfitting, *Journal of Machine Learning Research* 15 (1) (2014) 1929–1958.

- [11] P. Molchanov, S. Tyree, T. Karras, T. Aila, J. Kautz, Pruning convolutional neural networks for resource efficient inference, in: International Conference on Learning Representations (ICLR), 2017.
- [12] J. Frankle, M. Carbin, The lottery ticket hypothesis: Finding sparse, trainable neural networks, in: International Conference on Learning Representations (ICLR), 2019.
- [13] H. Li, A. Kadav, I. Durdanovic, H. Samet, A. P. Graf, Pruning filters for efficient convnets, in: International Conference on Learning Representations (ICLR), 2016.
- [14] N. Lee, T. Ajanthan, P. H. Torr, Snip: Single-shot network pruning based on connection sensitivity, in: International Conference on Learning Representations (ICLR), 2019.
- [15] C. Wang, G. Zhang, R. Grosse, Picking winning tickets before training by preserving gradient flow, in: International Conference on Learning Representations, 2020.
- [16] G. Chechik, I. Meilijson, E. Ruppin, Neuronal pruning in response to resource constraints, *Neural Computation* 11 (8) (1999) 2065–2083. doi:10.1162/089976699300016019.
- [17] Y. LeCun, Y. Bengio, G. Hinton, Pathways towards machine intelligence, *Communications of the ACM* 64 (8) (2021) 58–67. doi:10.1145/3448250.
- [18] M. Zhu, S. Gupta, To prune, or not to prune: Exploring the efficacy of pruning for model compression, in: arXiv preprint arXiv:1710.01878, 2017.
- [19] J. Zhu, R. D. Blakely, W. A. Hewlett, Mechanisms of synaptic pruning in the developing nervous system, *Current Opinion in Neurobiology* 45 (2017) 94–102. doi:10.1016/j.conb.2017.03.005.
- [20] D. B. Chklovskii, B. W. Mel, K. Svoboda, Cortical rewiring and information storage, *Nature* 431 (7010) (2004) 782–788. doi:10.1038/nature03012.

- [21] D. P. Kingma, T. Salimans, M. Welling, Variational dropout and the local reparameterization trick, in: Advances in Neural Information Processing Systems, Vol. 28, 2015.
- [22] Y. Gal, A. Kendall, Concrete dropout, Advances in Neural Information Processing Systems 30 (2017).
- [23] Larxel, S&p 500 stocks (daily updated), accessed: 19 May 2025 (2024).  
URL <https://www.kaggle.com/datasets/andrewmvd/sp-500-stocks>
- [24] Zielak, Bitcoin historical data, accessed: 19 May 2025 (2025).  
URL <https://www.kaggle.com/datasets/mczielinski/bitcoin-historical-data>
- [25] UCI Machine Learning, Household electric power consumption, accessed: 19 May 2025 (2016).  
URL <https://www.kaggle.com/datasets/uciml/electric-power-consumption-data-set>
- [26] Fedesoriano, Air quality dataset, accessed: 19 May 2025 (2020).  
URL <https://www.kaggle.com/datasets/fedesoriano/air-quality-data-set>
- [27] Y. Gal, Z. Ghahramani, Dropout as a bayesian approximation: Representing model uncertainty in deep learning, in: M. F. Balcan, K. Q. Weinberger (Eds.), Proceedings of The 33rd International Conference on Machine Learning, Vol. 48 of Proceedings of Machine Learning Research, PMLR, New York, New York, USA, 2016, pp. 1050–1059.  
URL <https://proceedings.mlr.press/v48/gal16.html>
- [28] T. V. Bliss, G. L. Collingridge, A synaptic model of memory: long-term potentiation in the hippocampus, *Nature* 361 (6407) (1993) 31–39.
- [29] M. F. Bear, R. C. Malenka, Synaptic plasticity: Ltp and ltd, *Current opinion in neurobiology* 6 (2) (1996) 169–173.
- [30] J.-P. Bourgeois, Synaptogenesis in the neocortex of the newborn: the ultimate frontier for individuation?, *Neurodevelopmental disorders* (1997) 91–113.
- [31] A. G. Howard, M. Zhu, B. Chen, D. Kalenichenko, W. Wang, T. Weyand, M. Andreetto, H. Adam, Movenets: Efficient convolutional neural networks for mobile vision applications, *arXiv preprint arXiv:1704.04861* (2017).

- [32] F. N. Iandola, S. Han, M. W. Moskewicz, K. Ashraf, W. J. Dally, K. Keutzer, SqueezeNet: Alexnet-level accuracy with 50x fewer parameters and 0.5 mb model size, in: arXiv preprint arXiv:1602.07360, 2016.
- [33] T. K. Hensch, Critical period regulation, *Annual review of neuroscience* 27 (2004) 549–579.
- [34] A. E. Takesian, T. K. Hensch, Balancing plasticity/stability across brain development, *Progress in brain research* 207 (2013) 3–34.